Journal of Power Technologies 101 (1) (2021) 34–43

A Comparative Study of Two Energy Management Schemes for a Fuel-cell Hybrid Power System of Four-Wheel-Drive Electric Vehicle

Mohammed Amine SOUMEUR[1,✉], Brahim GASBAOUI[1], Mohammed Amine HARTANI[1], and Othmane ABDELKHALEK[1]

[1]Tahri Mohammed University of Bechar, Smart Grid and renewable energy Laboratory
[✉]amirehamo@gmail.com

Abstract

This papers investigates energy management strategies (EMSs) for the hybrid Proton Exchange Membrane (PEM) Fuel Cell four-wheel-drive electric vehicle (4WDEV). A comparative study of two EMSs for 4WDEV hybrid powertrain source was carried out with a view to improving the vehicle's dynamic response during transients and minimizing hydrogen consumption. Three distributed energy resources (DERs), with the PEM Fuel Cell as the primary source, power the 4WDEV vehicle. A hybrid energy storage system (HESS) includes batteries and supercapacitor devices as the backup unit, in addition to covering autonomy hours. The proposed EMS aims to ensure optimal operation of the vehicle at variable motor speed and torque, taking into consideration the boundaries of the storage devices such as the states of charge and the DC bus voltage.

Keywords: Electric vehicle, Energy management, PEM Fuel cell, DTC-SVM, DC-DC converter, Hybrid storage

1 Introduction

The use of environmentally-friendly traction systems is increasing, especially in the transport sector. Fuel cells are being used in cars, buses, tramways, trains, and aircraft (Wu and Gao; Bauman and Kazerani; Schaltz and Rasmussen). Compared with conventional internal combustion engines, they provide electrical power with high efficiency, less noise and near-zero emissions (Renouard-Vallet; Roboam and Andrade; Jiang and Fahimi). To improve the dynamics of the electric vehicle and power density of fuel cell systems, we should hybridize fuel cells with energy storage or hybrid energy storage devices, such as lithium-ion batteries, supercapacitors or batteries/supercapacitor. This combination or hybridization delivers high performance dynamics for the electric vehicle. Nevertheless, the batteries/supercapacitors and the fuel cell system can be optimized to achieve better fuel economy, accomplished through an energy management strategy (EMS), which distributes load power among the energy sources (P. Garcia and Jurado). The EMS and power source components affect vehicle performance and fuel economy considerably in hybrid vehicles, because of the multiple power sources and differences in their characteristics (P. Garcia and Jurado; Dusmez and Khaligh; Caux and al.; Chun-Yan and Guo-Ping; Zhang; Vural; Soumeur). Also important are the various topologies of coupled multipower sources and different techniques of power management. Therefore, to minimize fuel consumption for a hybrid vehicle, optimal energy management and component sizing should be determined as a combined package. In this paper, a hybrid four-wheel-drive electric vehicle (4WDEV) is used and is described in Figure 1. Four induction motors deliver high stability on the road movement through four wheels. This 4WDEV is powered by hybrid power sources via a PEM fuel cell and hybrid storage, provided by battery and supercapacitor. Two different energy management systems were investigated with a view to improving vehicle performance dynamics and minimizing fuel consumption.

These strategies were compared and their advantages are highlighted below. The general configuration of the hybrid powertrain system as shown in Figure 2. The power system is composed of a fuel cell connected through the appropriate DC-DC boost converter, a battery connected via a bidirectional buck-boost converter and supercapacitor connected directly to the same DC bus. This hybrid power source is proposed to power a four in-wheel drive electric vehicle. Matlab Simulink was used to perform a simulation of this system and all results are given and interpreted.

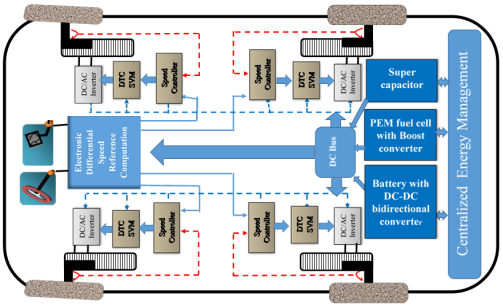

Figure 1: Proposed hybrid four-wheel-drive electric vehicle configuration

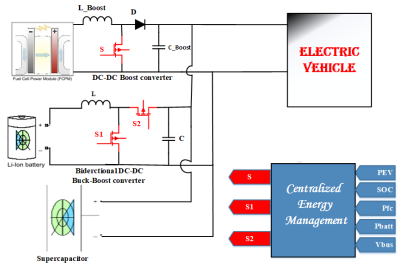

Figure 2: General configuration of the hybrid powertrain system

2 Electric vehicle description

The electric vehicle is influenced by many opposing forces, as shown in Figure 3. These forces are: rolling resistance force F_{tire} due to friction of the tires on the road; aerodynamic drag force F_{aero} caused by friction on the body moving through the air ; and climbing force F_{slope} dependent on the slope of the road (Bauer; Duffy and Stockel).

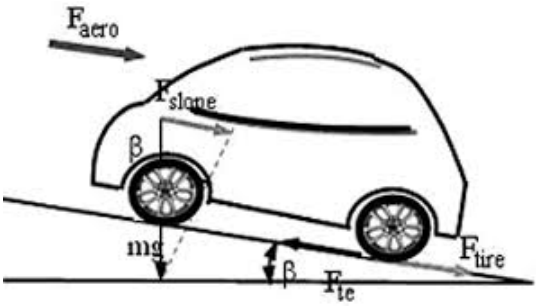

Figure 3: Forces acting on a vehicle.

We can define rolling resistance force by:

$$F_{tire} = Mgf_r \cos(\beta)$$

Aerodynamic resistance torque is given by the relationship below:

$$F_{aero} = \frac{1}{2}\rho_{air} A_f C_d v^2$$

Climbing force is usually modelled as:

$$F_{slope} = Mg \sin(\beta)$$

Total resistive force is equal to the sum of all resistance forces, as shown below:

$$F_r = F_{tire} + F_{aero} + F_{slope}$$

For sizing electric vehicle energy source, it is important to estimate the required power of the electric vehicle by using the following relationship, expressed by (Allaoua; Wang and Fang; Mebarki):

$$P_{Load} = v(\frac{1}{2}\rho_{air} \cdot v^2 \cdot A_f \cdot C_d + M \cdot g \cdot f_r + M\frac{dV}{dt})$$

where : M—Total vehicle mass, kg; v—Vehicle speed, m/s; A_f—vehicle frontal area, area,m^2; C_d—Aerodynamic drag coefficient, m/s; ρ_{air}— Air density, kg/m^3; B— the road slope angle, degree°; r—tire radius, m; g—gravity acceleration, m/s^2. The values of these parameters are shown in Table 1.

r (m)	m(kg)	f_r
0.32	1400	0.01
A_f **(m^2)**	C_d	ρ_{air} **(Kg/m^3)**
2.61	0.32	1.11

Table 1: Parameters of the electric vehicle model

3 Fuel cell model and description

Fuel cells transform chemical energy into electrical energy in a straightforward way, by oxidizing hydrogen. PEMFCs are the preferred in-car application, compared to others. Typically, PEMFCs are productive and compact (Tirnovan; Marsala; Methekar; Radisavljevic)(Tirnovan; Marsala; Methekar; Radisavljevic). The fuel cell stack parameters chosen are shown in Table 2.

Cell potential is calculated by using the sum of losses in the following equation:

$$V_{FC} = E_{nerst} + V_{act} + V_{ohmic} + V_{con}$$

where

$$E = 1.229 - [(\frac{RT}{nF})\ln(\frac{P_{H2O}}{P_{H2}\cdot\sqrt{P_{O2}}})]$$

$$V_{act} = \xi_1 + \xi_2 T + \xi_3 T \ln \mathrm{Co}_2 + \xi_4 T \ln \mathrm{I}_{FC}$$

$$V_{ohmic} = -I_{FC} R_m$$

$$R_m = \frac{\rho_m l_m}{A}$$

$$V_{con} = B(1 - \frac{I_{FC}}{I_{L\max} A})$$

Stack voltage was calculated assuming a nominal operating voltage of 0.72V per cell. The fuel stack system includes an H2 controller and O2 controller, which regulate the flow rate of H2 and the flow rate of O2, respectively, by using the relationships below:

$$Uf_{H_2} = \frac{60000 R T I_{FC}}{2F P_{fuel} V_{fuel} x}$$

$$Uf_{O_2} = \frac{60000 R T I_{FC}}{4F P_{air} V_{air} y}$$

where: R—Ideal gas constant, J/mol/K; T—Stack temperature, °C; I_{fc} —Fuel cell current, A; F—Faraday constant, A.s/mol; P_{Air} —Air inlet pressure, bar; V_{Air} —Air flow rate, l/min; y—Nominal composition of oxygen, %; x—Nominal composition of hydrogen, %; P_{fuel}—Fuel pressure, bar; V_{fuel}—Fuel flow rate, l/min; P_{H2}—Hydrogen partial pressure, atm; P_{O2}—Oxygen partial pressure, atm; Uf_{O2}—oxygen utilization, % ; Uf_{H2}—Hydrogen utilization, %.

Parameter	value
Open circuit voltage (V)	400
Nominal operating point (A,V)	I=200 ,V=250
Maximum operating point (A,V)	Imax=300, Vmax=300
Number of cells	334
Nominal stack efficiency(%)	55
Nominal air flow rate (lpm)	2100
Nominal supply pressure (bar)	H2:15 , Air: 1
Operating temperature (C°)	65
Nominal composition (%)	H2:9995 , O2:21 , H2O(Air): 1

Table 2: Fuel cell stack parameters

4 Supercapacitor model

The use of supercapacitors in hybrids is imperative, due to their quick reaction. For energy capacity, it is crucial to have numerous cells (series/parallel) to obtain a high level of voltage and current since SC contains a very low voltage. Figure 4 represents the model used, which includes an internal resistance RL and equivalent capacitor Cv, (Uzunoglu and Alam; Camara). The supercapacitor model is presented in equation (14).

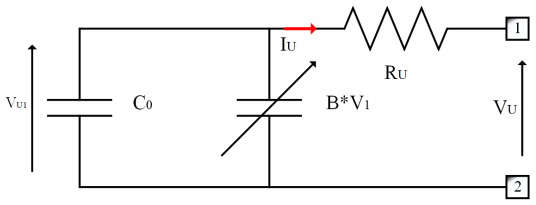

Figure 4: Supercapacitor model scheme

$$\begin{cases} amp; V_U = V_{U_1} - R_U \cdot I_U \\ amp; I_U = \pm\frac{dQ_u}{dt} \\ amp; C_U = C_0 + \beta \cdot V_{U_1} \\ amp; \frac{dV_{U_1}}{dt} = K \cdot \frac{I_U}{(C_0 + 2\cdot\beta\cdot V_{U_1})} \end{cases}$$

5 Battery model

Numerous electrical models are available in the litterature that depict the dynamic behavior of the battery and the electrochemical processes (Coleman and Lee.; Chen; Stockar). In this work the lithium battery is utilized, as seen in Figure 5 . This model includes an equilibrium voltage VEMF, which reflects the state of charge (SoC), inner resistance R, and a parallel RC circuit which portrays the charge exchange, and the diffusion handle between the cathode and the electrolytes.The mathematical model of the lithium battery is presented in the following equation:

$$\begin{cases} amp; V_{LB} = V_{EMF} - Z \times I_{LB} \\ amp; Z = R_\Omega + \frac{R_C}{1 + \tau \times s} \end{cases} \qquad \tau = C_C \times R_C$$

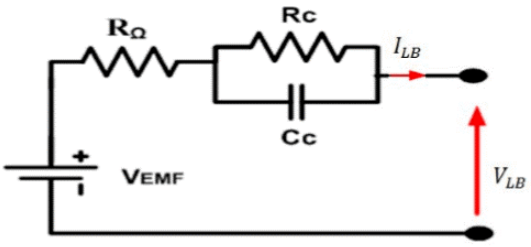

Figure 5: Lithium battery model

6 Direct torque control strategy based space vector modulation (DTC-SVM)

DTC-SVM strategies operate at a constant switching frequency, this type of control strategy depending on the applied flux and torque control algorithm. Basically, the controllers calculate the required stator voltage vector and then it is realized by space vector modulation technique, (ianguo and Quanshi; Arunadevi). This technique is built by two PI controllers, to control the torque and the volume of the flux, as seen in Figure 6. Referring to Figure 6, two relative necessarily (PI) sort controllers direct the flux volume and the torque, individually. Hence, both the torque and the size of flux are below control, subsequently creating the voltage command for inverter control. No decoupling instrument is required, as the flux volume and the torque can be controlled by the PI controllers, (ianguo and Quanshi; Arunadevi; Zhang; Brandstetter and Palacky).

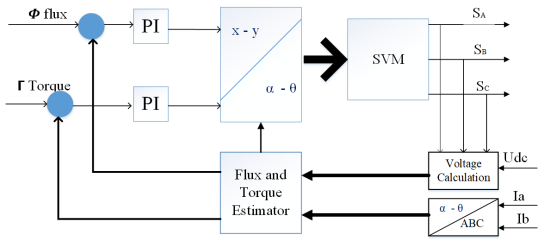

Figure 6: General diagram of DTC-SVM strategy

7 Energy management

7.1 Classical PI strategy

In this energy management strategy, the battery SOC is controlled using a PI controller, which is afterwards removed from the required power by the electric vehicle to obtain the fuel cell reference power, as shown in Figure 7 (Motapon and Al-Haddad; Li; Thounthong and Rael). When the battery SOC is lower than the reference (SOCmin), the fuel cell power is low and the battery gives full power. When the SOC is below the reference, the fuel cell provides almost the required electric vehicle power. This method is described by Flowchart in Figure 8.

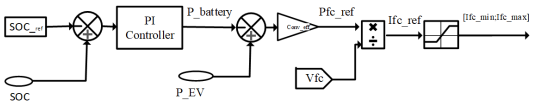

Figure 7: Classical PI energy management strategy

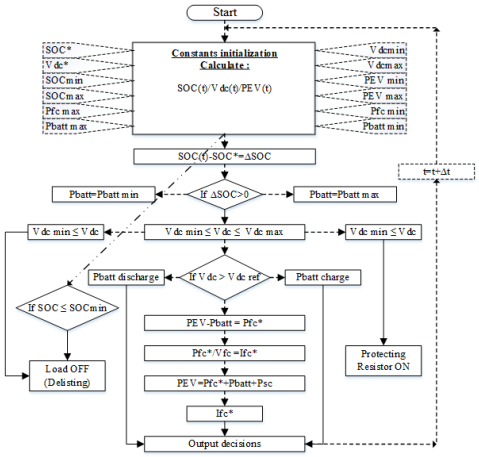

Figure 8: Flow chart of classical PI method

7.2 State machine strategy

This energy management strategy (state machine) consists of twelve states, as shown in Figure 9 Figure 9 (a), and is built by using the same approach as proposed in (Fernandez et al. (2011). It is based on hysteresis as it moves between all twelve states. When the states number is increasing, this technique gives good results due to the slow reaction of the method (Motapon and Al-Haddad) (Chun-Yan and Guo-Ping; Chen and Tsai; Vural).

Fuel cell power is decided based on the battery SOC run and required vehicle power. Figure 9 (b) is required when exchanging states, which influences the reaction of the EMS to changes in power demanded

by the vehicle. To solve this problem or improve the efficiency of this strategy, the number of states must be increased.

A general overiew of this technique is presented in Figure 10. As input two parameters are entered: required power and battery SOC. After calculation by using the management algorithm, we obtain as output the reference fuel cell power, which divided by the fuel cell voltage gives the reference fuel cell current. The flowchart of this strategy is given in Figure 11.

if SOC High	and if PEV < Pmin	state 01	Pfc*=PEV+Pbatt_charmax
if SOC High	and if PEV∈ [Pmin ; Pmax]	state 02	Pfc*= PEV
if SOC High	and if PEV >Pmax	state 03	Pfc*= PEV+Pbatt_charvar
if SOC Inormal	and if PEV < Pmin	state 04	Pfc*= PEV+Pbatt_charmax
if SOC Inormal	and if PEV∈ [Pmin ; Pmax]	state 05	Pfc*= PEV-Pbatt_charmax
if SOC Inormal	and if PEV >Pmax	state 06	Pfc*= PEV-Pbatt_charvar
if SOC Normal	and if PEV < Pmin	state 07	Pfc*= PEV+Pbatt_charmax
if SOC Normal	and if PEV∈ [Pmin ; Pmax]	state 08	Pfc*= PEV-Pbatt_charmax
If SOC Normal	and if PEV >Pmax	state 09	Pfc*= PEV+Pbatt_charvar
If SOC Low	and if PEV < Pmin	state 10	Pfc*=PEV+Pbatt_charmax
If SOC Low	and if PEV∈ [Pmin ; Pmax]	state 11	Pfc*=PEV+ Pbatt_charvar
If SOC Low	and if PEV >Pmax	state 12	Pfc*=PEV

SOC High ⟶ SOC > SOCmax; SOCmax=90; SOCmin=30; SOCmid=50
SOC Inormal ⟶ SOC ∈ [SOCmin, SOCmid]; Pmin=10e3; Pmax=50e3
SOC Normal ⟶ SOC ∈ [SOCmid, SOCmax]; Pbatt_charmax=10e3
SOC Low ⟶ SOC < SOCmin; Pbatt_charvar=min (10e3, 50e3-u (1))

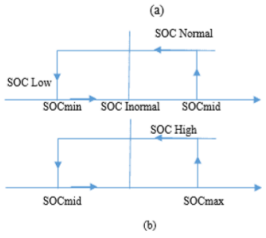

Figure 9: (a) State machine control decisions and (b) Hysteresis control

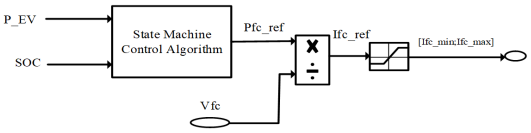

Figure 10: General overview of the state machine method

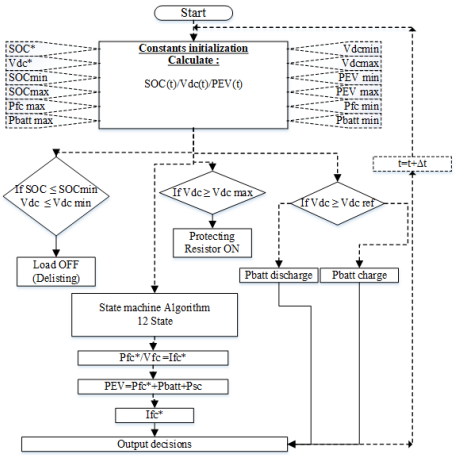

Figure 11: Flowchart of the state machine Method

8 Results and discussion

In order to characterize the behavior of the 4WDEV electric vehicle and the power evolution of the hybrid system and to see the influence of two methods of energy management, we made an electric vehicle trajectory divided into six phases:

1. At 0 to 11 s the car travels at 80 km / h with transitory phase for 0 km/h to 80 km/h.
2. At 11 to 16 s the car increases speed to 150 km /h
3. At 16 to 21 s At this interval, the car crosses a ramp of 10 degrees with a speed of 150 km / h
4. At 21 s the slope ends with the car at 150 km/h to 25 s.
5. At 25 s, the car decelerates to 100 km /h and stays stable to 35 s.
6. At 35 s the speed drops directly to 20 km/h and stays stable to 45 s.

MATLAB / SIMULINK is utilized to simulate and test the proposed model of the Hybrid 4WDEV, and to apply two energy management startegies. This showed us the performance of 4WDEV with four induction motors, controlled by a direct torque controller with space state vector technique (DTC-SVM), at various speeds on the proposed trajectory. It showed us the behaviors of the electric vehicle power, fuel cell power and SC power, and additionally the battery SOC, fuel consumption and DC bus voltage under different energy management. The motor parameters used are given in Table 3.

The vehicle's speed is presented in Figure 12. We note that it follows the reference speed in all the phases we proposed, with good reaction, without overshoot (pic) and with almost negligible ripple.

Parameter	Type or Value
Motor	Indction Motor
Input voltage	400 volt
Max output power	15 kw for one motor
Output torque	(100 + 100)
Control mode	DTC-SVM

Table 3: Parameter of the used motor

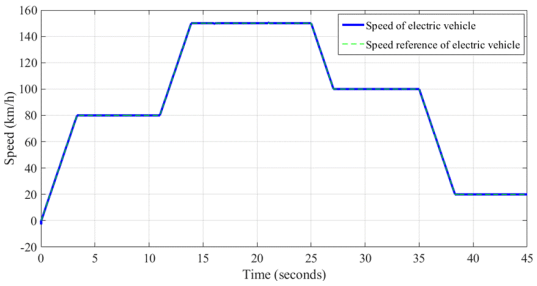

Figure 12: Electric vehicle speed

The simulation results are divided in two:

Firstly, the Classical PI method simulation results:

Figure 13 depicts the power evolution of fuel cell power, the required electric vehicle power, battery power and the supercapacitor power in all phases. After seeing these results, we noted great demand in the required electric vehicle power at the start, which explains the starting torque of the four induction motors, so in this case the supercapacitor and the battery help the fuel cell and provide the missing power caused by the slow response of the fuel cell. After the overshoot power demand of starting, we see a drop in the required power, but the battery and supercapacitor are charging with the remaining power of the fuel cell because it is decreasing slowly and it has minimal power limited in 6e3 watt. After this the electric vehicle arrives at the permanent state at 2.6 s to 11 s. In these phases SC power equals zero, because the 4WDEV is at steady state, but the battery tries to give a little power to help the fuel cell. In the second phase, 4WDEV's speed is increased from 80 km/h to 150 km/h after a transitional state, the vehicle stays at the same speed of 150 km/h to 25 s. Following this increase, the required power also increases and the fuel cell provides this demand. At 17 seconds the vehicle enters a ramp of 30 degrees and this variation causes an increase in required power, because of the increase in resistor torque. Therefore the fuel cell increases the power given to 50e3 watt, which is the nominal power to furnish this demand. However, in this case the electric vehicle demands greater power than the power of the fuel cell, and the battery provides the missing power. The supercapacitor gives a negative or positive overshoot in each rapid variation in speed (acceleration, deceleration and braking) or resistor torque (ramp, slope) to keep the electric vehicle stable. In the third phase the required power decreases from 45e3 watt to 17e3 watt due to the speed slowing from 150 km to 100 km/h. The fuel cell gives the power to meet this requirement. At 27 s the steady-state of the third phase starts, in this case the battery helps the fuel cell by almost 2e3 watt to supply the electric vehicle (discharging the battery). Finally, the 4WDEV arrives at the fourth phase and we see the drop in required power to the minimal power of the fuel cell 7e3 watt which describes the rapid deceleration of the electric vehicle. We see at this point that the required power is less than the power given by the fuel cell. Therefore the battery is charging up with the remaining power. The supercapacitor, too, gave overshoot power during any rapid variation.

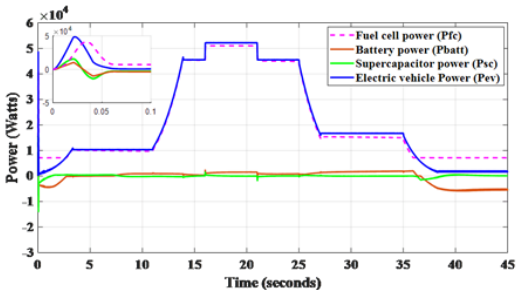

Figure 13: Power evolution under all phases

The DC bus voltage of the 4WDEV is shown in Figure 14, where we notice it follows the reference 400 volts in all phases with the rapid response time of 0.04 s, with a small ripple of 3 volts and an overshoot of 7 volt. After we saw the DC bus voltage, we noted the influence of each phase on the DC bus, but as the control is effective the 4WDEV remains in good operation.

Figure 15 illustrates the 4WDEV battery SOC in all phases, where it is charged and discharged depending on the power balance.

In Figure 16, the consumption and fuel-air ratio are depicted. Consumption goes up along with every increase in required power. Maximum fuel consumption is 380 from 400 lpm and air consumption is 1400 from 2200 lpm.

Secondly, the simulation results of the state machine method:

In this technique too we tested management by the same trajectory as used in the first method, so all results are given in the following charts:

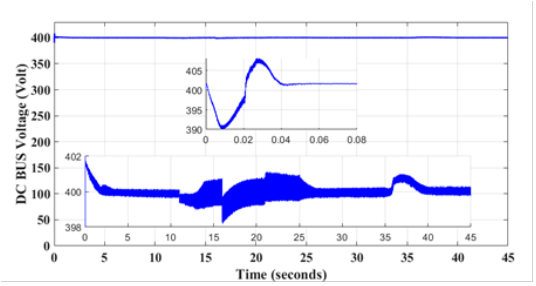

Figure 14: DC bus voltage in all phases

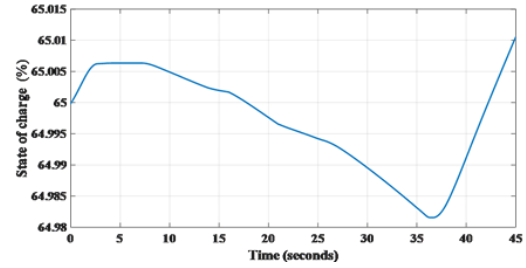

Figure 15: Battery state of charge in all phases

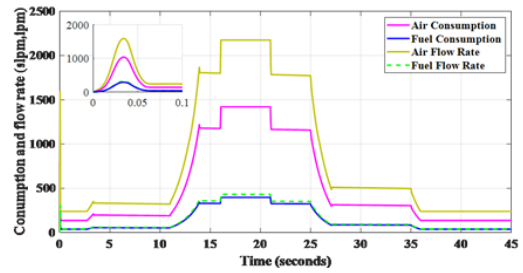

Figure 16: The flow rate and consumption of fuel-air in all phases

Figure 17 illustrates the power evolution of the fuel cell, battery, supercapacitor and the required electric vehicle power, in the whole trajectory. We noticed high power demand by the vehicle at the start of the trajectory, because of the starting torque. We saw the fuel cell supply the 4WDEV and it charged the battery by the maximum power possible,10 kwatt from 0 to 13 s. After this the battery power charging decreases on account of the fuel cell approaching the nominal power appointed the limited power in this management strategy. At 17 s the 4WDEV enters a ramp of 30 degree, increasing the required power. However, the fuel cell reduces the given power owing to the management condition, therefore the battery discharging provides the missing power in this system from 17 to 22 s, the ramp end. The supercapacitor gives a negative or positive overshoot during any rapid variation (drop or overshoot) to make the vehicle stable. From 22 s to the trajectory end, the fuel cell supplies the required power and charges the battery by the maximum power possible.

Figure 18 depicts the DC bus voltage of the 4WDEV where we noticed it follows the reference 400 volts with an overshoot of 10 volt and rapid response time of 0.05 s and with almost negligible ripple, so we can conclude that the control management is efficient.

The battery SOC in the whole trajectory is shown in Figure 19. It is charged by the fuel cell and discharged to provide missing power, this operation depends on the power balance and energy management strategy. We saw the battery charged from 0 to 17 s and from 22 to the trajectory end, and it is discharged from 17 to 22 s.

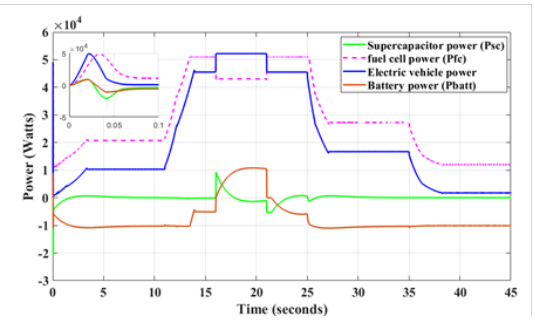

Figure 17: Power evolution in the whole electric vehicle trajectory

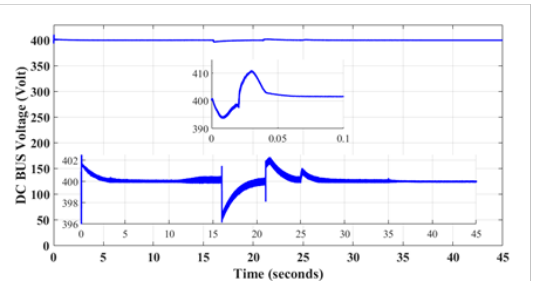

Figure 18: DC bus voltage in the whole electric vehicle trajectory

Figure 20 depicts the consumption and flow rate of fuel-air. We noticed a rise in consumption at every increase in required power, but when the power increases to higher than 50e3 watt, the fuel and air consumption decreases, the maximum fuel consumption is 350 from 400 lpm and air consumption is 1400 from 2200 lpm. Consumption in this strategy depends on the power balance and the condition that we set up.

The results of these two energy management strategies: classical PI and state machine were put in Table 4 for comparison purposes. Each strategy has

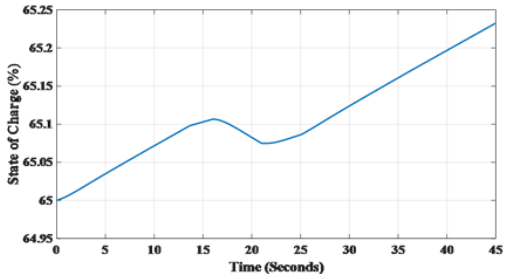

Figure 19: Battery state of charge in the whole electric vehicle trajectory

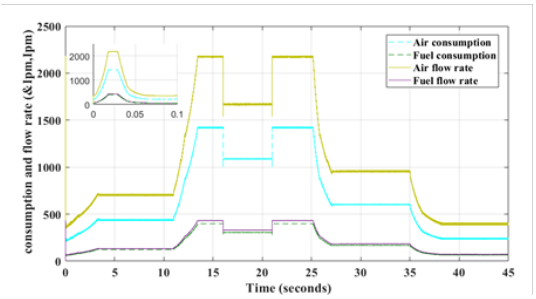

Figure 20: Flow rate and consumption of fuel-air in the whole electric vehicle trajectory

advantages and disadvantages: the classical PI technique has a faster response time and a smaller overshoot than the state machine strategy, but the drawback of Classical PI it that it is work without a condition and algorithm. This makes the system work with several conditions. The state machine strategy allows you to adopt several conditions and optimize fuel as you wish, but it is has a drawback in its slow response to the idea of work.

	Classical PI strategy
State of charge (%)	From 6498 to 65006
Response time (s)	0.04
Overshoot (V)	7
Ripple (V)	3
Fuel consumption (%)	21
Air consumption (%)	27.7
	State machine Strategy
State of charge (%)	From 65 to 6525
Response time (s)	0.05
Overshoot (V)	10
Ripple (V)	0
Fuel consumption (%)	30.12
Air consumption (%)	39.67

Table 4: Comparison between classical PI and state machine strategies

9 Conclusions

This work focuses on the energy management strategy and behavior of a hybrid four-wheel-drive electric vehicle powered by battery, PEM fuel cell and supercapacitors connected by converters. Moreover, we present modelling of the behavior of energy sources, and two energy management strategies (Classical PI and state machine). The simulation tests these energy management strategies and shows the operation of the hybrid energy source, where we determine the energy management strategies to help improve electric vehicle operation and to minimize fuel consumption.

10 Acknowledgments

The authors are thankful to the Director-General for Scientific Research and Technological Development, DGRSDT for providing a research grant.

References

Allaoua, B. *Vehicle Tout* $_{E}electrique_{A}Sourced'_{E}nergieHybrideLithium - Ion/FCPEM.Allemagne$, 2017.

Arunadevi, et al, R. "Analysis of Direct Torque Control Using Space Vector Modulation for Three Phase Induction Motor". Recent Research in Science and Technology, vol. 7, no. 3, 2011.

Bauer, Horst. Automotive Handbook. American Educational Systems, 1986.

Bauman, Jennifer, and Mehrdad Kazerani. "A Comparative Study of Fuel-Cell–Battery, Fuel-Cell–Ultracapacitor, and Fuel-Cell–Battery–Ultracapacitor Vehicles". IEEE Transactions on Vehicular Technology, vol. 57, no. 2, March 2008, pp. 760–69.

Brandstetter, Petr Chlebis, Pavel, and Petr Palacky. "Direct Torque Control of Induction Motor with Direct Calculation of Voltage Vector". Advances in Electrical and Computer Engineering, vol. 10, no. 4, 2010, pp. 17–22.

Camara, et al, Mamadou Baïlo. "DC/DC Converter Design for Supercapacitor and Battery Power Management in Hybrid Vehicle Applications—Polynomial Control Strategy". IEEE Transactions on Industrial Electronics, vol. 57, no. 2, 2010, pp. 587–97.

Caux, S., and al. "On-Line Fuzzy Energy Management for Hybrid Fuel Cell SystemOn-Line Fuzzy Energy Management for Hybrid Fuel Cell Systems". In-

ternational Journal of Hydrogen Energy, vol. 35, no. 5, 2010, pp. 2134–43.

Chen, Liang-Rui. "Design of Duty-Varied Voltage Pulse Charger for Improving Li-Ion Battery-Charging Response". IEEE Transactions on Industrial Electronics, vol. 56, no. 2, 2009, pp. 480–87.

Chen, Yuh-Yih Wu, Bo-Chiuan, and Hsien-Chi Tsai. "Design and Analysis of Power Management Strategy for Range Extended Electric Vehicle Using Dynamic Programming". Applied Energy, vol. 113, 2014, pp. 1764–74.

Chun-Yan, L., and L. Guo-Ping. "Optimal Fuzzy Power Control and Management of Fuel Cell/Battery Hybrid Vehicles". Journal of Power Sources, vol. 192, no. 2, 2009, pp. 525–33.

Coleman, William Gerard Hurley, Martin, and Chin Kwan Lee. "An Improved Battery Characterization Method Using a Two-Pulse Load Test". IIEEE Transactions on Energy Conversion, vol. 23, no. 2, 2008, pp. 708–13.

Duffy, M. T. Stockel, J. E., and M. W. Stockel. Automotive Mechanics Fundamentals. How and Why of the Design, Construction, and Operation of Modern Automotive Systems and Units, 1988.

Dusmez, Serkan, and Alireza Khaligh. "A Supervisory Power-Splitting Approach for a New Ultracapacitor–Battery Vehicle Deploying Two Propulsion Machines". EEE Transactions on Industrial Informatics, vol. 10, no. 3, 2014, pp. 1960–71.

Jiang, Wei, and Babak Fahimi. "Active Current Sharing and Source Management in Fuel Cell–Battery Hybrid Power System". IEEE Transactions on Industrial Electronics, vol. 57, no. 2, 2009, pp. 752–61.

Li, et al, Qi. "Energy Management Strategy for Fuel Cell/Battery/Ultracapacitor Hybrid Vehicle Based on Fuzzy Logic". International Journal of Electrical Power & Energy Systems, vol. 43, no. 1, 2012, pp. 514–25.

Marsala, et al, Giuseppe. "A Prototype of a Fuel Cell PEM Emulator Based on a Buck Converter". Applied Energy, vol. 86, no. 10, 2009, pp. 2192–203.

Mebarki, et al, Nasser. "PEM Fuel Cell/Battery Storage System Supplying Electric Vehicle". International Journal of Hydrogen Energy, vol. 45, no. 41, 2016, pp. 20993–1005.

Methekar, et al, R. N. "Control of Proton Exchange Membrane Fuel Cells Using Data Driven State Space Models.". Chemical Engineering Research and Design, vol. 88, no. 7, 2010, pp. 861–74.

Motapon, Louis-A. Dessaint, Souleman Njoya, and Kamal Al-Haddad. "A Comparative Study of Energy Management Schemes for a Fuel-Cell Hybrid Emergency Power System of More-Electric Aircraft". IEEE Transactions on Industrial Electronics, vol. 61, no. 3, 2013, pp. 1320–34.

P. Garcia, C. A. Garcia, L. M. Fernandez, and F. Jurado. "Energy Management System of Fuel-Cell-Battery Hybrid Tramway". IEEE Transactions on Industrial Electronics, vol. 57, no. 12, 2010, pp. 4013–23.

Radisavljevic, Verica. "On Controllability and System Constraints of the Linear Models of Proton Exchange Membrane and Solid Oxide Fuel Cells". Journal of Power Sources, vol. 196, no. 20, 2011, pp. 8549–52.

Renouard-Vallet, et al, Gwénaëlle. "Improving the Environmental Impact of Civil Aircraft by Fuel Cell Technology: Concepts and Technological Progress". Energy & Environmental Science, vol. 3, no. 10, 2010, pp. 1458–68.

Roboam, Bruno Sareni, Xavier, and Andre De Andrade. "More Electricity in the Air: Toward Optimized Electrical Networks Embedded in More-Electrical Aircraft". IEEE Industrial Electronics Magazine, vol. 6, no. 4, December 2012, pp. 6–17.

Schaltz, Alireza Khaligh, Erik, and Peter Omand Rasmussen. "Investigation of Battery/Ultracapacitor Energy Storage Rating for a Fuel Cell Hybrid Electric Vehicle". IEEE Vehicle Power and Propulsion Conference, 2008.

Soumeur, et al, Mohammed Amine. "Energy Management for a Hybrid Fuel Cell/SC for Four-Wheel Drive Electric Vehicle". Electrotehnica, Electronica, Automatica, vol. 67, no. 3, 2019, pp. 58–64.

Stockar, et al, Stephanie. "Energy-Optimal Control of Plug-in Hybrid Electric Vehicles for Real-World Driving Cycles". IEEE Transactions on Vehicular Technology, vol. 60, no. 7, 2011, pp. 2949–62.

Thounthong, Phatiphat, and Stephane Rael. "The Benefits of Hybridization". IEEE Industrial Electronics Magazine, vol. 3, 2009.

Tirnovan, et al, R. "Surrogate Modelling of Compressor Characteristics for Fuel-Cell Applications". Applied Energy, vol. 85, no. 5, 2008, pp. 394–403.

Uzunoglu, M., and M. S. Alam. "Modeling and Analysis of an FC/UC Hybrid Vehicular Power System Using a Novel-Wavelet-Based Load Sharing Algorithm". IEEE Transactions on Energy Conversion, vol. 23, no. 1, 2008, pp. 263–72.

Vural, et al, Bülent. "Fuel Cell and Ultra-Capacitor

Hybridization: A Prototype Test Bench Based Analysis of Different Energy Management Strategies for Vehicular Applications". International Journal of Hydrogen Energy, vol. 35, no. 20, 2010, pp. 11161–71.

Wang, Fu-Cheng, and Wei-Hung Fang. "The Development of a PEMFC Hybrid Power Electric Vehicle with Automatic Sodium Borohydride Hydrogen Generation". International Journal of Hydrogen Energy, vol. 42, no. 15, 2017, pp. 10376–89.

Wu, Ying, and Hongwei Gao. "Optimization of Fuel Cell and Supercapacitor for Fuel-Cell Electric Vehicles". IEEE Transactions on Vehicular Technology, vol. 55, no. 6, November 2006, pp. 1748–55.

Zhang, et al, Zhifeng. "Novel Direct Torque Control Based on Space Vector Modulation with Adaptive Stator Flux Observer for Induction Motors". IEEE Transactions on Magnetics, vol. 46, no. 8, 2010, pp. 3133–36.

Zhang, et al., Xi. "Wavelet-Transform-Based Power Management of Hybrid Vehicles with Multiple on-Board Energy Sources Including Fuel Cell, Battery and Ultracapacitor". Journal of Power Sources, vol. 185, no. 2, 2008, pp. 1533–43.

ianguo, Song, and Chen Quanshi. "Research of Electric Vehicle IM Controller Based on Space Vector Modulation Direct Torque Control". 2005 International Conference on Electrical Machines and Systems, vol. Vol. 2, 2005.